General Disclaimer

One or more of the Following Statements may affect this Document

- This document has been reproduced from the best copy furnished by the organizational source. It is being released in the interest of making available as much information as possible.

- This document may contain data, which exceeds the sheet parameters. It was furnished in this condition by the organizational source and is the best copy available.

- This document may contain tone-on-tone or color graphs, charts and/or pictures, which have been reproduced in black and white.

- This document is paginated as submitted by the original source.

- Portions of this document are not fully legible due to the historical nature of some of the material. However, it is the best reproduction available from the original submission.

E83-10034
CR-169507

THE MINERALOGY OF GLOBAL MAGNETIC ANOMALIES

PROGRESS REPORT

FEBRUARY 1982 - AUGUST 1982

PROJECT MAGSAT

NATIONAL AERONAUTIC AND SPACE ADMINISTRATION

GODDARD SPACE FLIGHT CENTER

GREENBELT, MARYLAND 20771

(E83-10034) THE MINERALOGY OF GLOBAL MAGNETIC ANOMALIES Progress Report, Feb. - Aug. 1982 (Massachusetts Univ.) 47 p HC A03/MF A01 CSCL 08G

N83-13528

Unclas
G3/43 00034

CONTRACT NUMBER: NAS5-26414

PRINCIPAL INVESTIGATOR: STEPHEN E. HAGGERTY

DEPARTMENT OF GEOLOGY

UNIVERSITY OF MASSACHUSETTS

AMHERST, MASSACHUSETTS 01003

AUGUST 13, 1982

CONTENTS

INTRODUCTION

Our participation in the MAGSAT mission is directed toward the aquisition of experimental and analytical data on the magnet mineralogy of crustal and upper mantle igneous and metamorphic rocks.

These data are fundamental to the development of realistic models of crustal magnetization and the interpretation of satellite magnetic anomaly maps. Our approach focuses on the determination of Curie temperatures, magnetic susceptibilities and magnetic mineral chemistries, with particular attention to lower crustal and upper mantle rocks. Experimental phase equilibria studies of oxide, sulphide and alloy stability fields are complementary in providing an integrated magnetic mineral data base for the interpretation of rock magnetization.

During the report period the Curie Balance has been brought to operational stage and is producing data of a preliminary nature, some of which provides the basis of this report. Substantial problems experience in the assembly and initial operation of the instrument have, for the most part, been rectified, but certain problems still exist. Relationsnips between the geology and the gravity and MAGSAT anomalies of West Africa are briefly reexamined in the context of a partial reconstruction of Gondwanaland.

PROGRESS REPORT

In the present configuration the Curie Balance can routinely measure susceptibility, intensity of induced magnetization, and the thermal decay of magnetization above room temperature. The experimental methods and standards we have adopted are illustrated with natural samples, following a brief description of the instrument. The majority of this report is devoted to the magnetic properties of a small group of kimberlitic ilmenites from Liberia, West Africa, as measured by the Curie Balance.

Aspects of an internally consistent geological and geophysical framework for the interpretation of MAGSAT anomalies over West Africa are briefly described in the second, and complementary, part of the report.

CURIE BALANCE

INSTRUMENTATION

The Cahn Magnetic Susceptibility System is based on the Curie or Faraday method, in which a balance measures the magnetization of an object by sensing its apparent changes in weight according to magnetic field intensity and the temperature. We have adapted the Cahn system as a traditional rock magnetic Curie Balance (e.g., Collinson et al., 1967; Schwarz, 1968).

The magnetic field is manually controlled between 10^6 and 40 A/m (about 10 kOe and .5 Oe) and is measured by a Hall Probe Gaussmeter. Isothermal experiments or limited temperature programming are possible between

ambient and 800°c; a Pt-Rh thermocouple in close proximity to the sample is referenced (±5°c) to materials of known Curie temperature. Analyses can be made in air, vacuum or Argon (99.999%) at controlled flow rates. A Cahn 2000 electrobalance measures apparent sample mass which is translated to magnetic intensity values.

For a typical 10 mg sample the resolution of the Curie Balance is accurate to about ±5% within the specific susceptibility range 10^{-7} to 10^{-1} cgs units per gm (10^{-4} to 10 S.I. volume susceptibility). The sensitivity is 10^{-9} Am^2 or 10^{-6} emu.

EXPERIMENTAL WORK

(A) Magnetization measurements.

The specific susceptibility is simply derived from the expression for force on the sample $F_z = mX_{gm}H_x dH_x/dz$ (e.g., Morris and Wold, 1965), provided that the quantity $H_x dH_x/dz$ is constant over the volume of the sample and its value is known. Such tedious measurements (e.g., Figure 1) give an "absolute" value for the magnetization.

An alternative method (Lindoy et al., 1972; Mulay, 1963) simply compares the magnitudes of the apparent weight changes of the unknown and reference susceptibility samples. This is the method we have so far employed, using $HgCo(CNS)_4$ of known susceptibility (Lindoy et al., 1963; Muller and Guntherodt, 1981).

Two magnetization curves, specific magnetization versus field strength, for the Holyoke Basalt are shown in Figure 2. The higher curve was measured in vacuuo, at 309°k at Bell Laboratories (J. Waszczak, pers. comm.) and compares closely to our curve measured on a sample split from

the same aliquot of powdered material, but measured in air at 307°k by the relative method.

The Holyoke Basalt material was donated from our Department of Geology X.R.F. Laboratory in-house geochemical standards collection, and provides a useful working magnetic standard by virtue of the results obtained at Bell Laboratories.

(B) Curie temperature measurements

A repeatable increasing temperature program of about 10°c per minute is possible with the apparatus, and the thermocouple millivoltage for the heating cycle has been temperature calibrated against metal alloy Curie point standards. Testing the calibration against high purity synthetic and natural pyrrhotite (320°c), magnetite (580°c) and hematite (680°c) we found Curie points within $\pm$5°c ($\pm$10°c for hematite) of the quoted value.

Heating and cooling cycles for the Holyoke Basalt in Figure 3 are traced directly from the chart record; note the non-linear temperature scale. The Holyoke Basalt typically contains titanomagnetite with abundant oxyexsolution laths of ilmenite; high temperature oxidation products such as rutile and titanohematite are not observed, but low temperature alteration to titanomaghemite is common (Gunter, 1978). The analyzed material has been vigorously crushed and powdered.

A single relatively well defined Curie point of about 575°c (Figure 5) confirms the presence of magnetite. A lower temperature straight line segment terminating at about 450°c may be reflecting the effect of titanomaghemite. The weight loss during the experiment is due to partial devolitilization of the rock.

Important information given by the degree of reversibility of the thermomagnetic curve (e.g., Radhakrishnamurthy and Likhite, 1970) is lost because we cannot program cooling rates, except manually. The cooling cycle does provide qualitative information on the number of magnetic phases and an accurate measurement of the change in room temperature magnetization due to the heat treatment.

Figure 4 compares the thermomagnetic curves for an unknown mixture of sulfides and the curve obtained by Schwarz (1974) for a known mixture of Fe_9S_{10} and Fe_7S_8. Both species are clearly present in our experimental sample. The sudden increase in magnetization on quench cooling the Fe_9S_{10} phase also explains why our specimen left the sample bucket on rapid cooling through the Fe_9S_{10} Curie point ($\simeq$ 270°c).

(C) Magnetic properties of selected kimberlitic ilmenites.

To test the analytical performance of the Curie Balance we selected fresh unweathered ilmenites of probable kilberlitic origin from Liberia, West Africa.

Room temperature magnetizations were measured as outlined above. Figure 5 shows specific susceptibility versus applied field strength for ilmenites KK-ILM-11 to 15, according to the method of Honda and Owen (Bates, 1963, p. 134) in which a line of positive slope indicates ferro- or ferrimagnetism. Sample 14 has constant susceptibility. KK-ILM-11 is plotted on a scale reduced by a factor of ten and is distinguished from the other samples in the range of magnitude of its susceptibility.

Initial magnetization curves are shown in Figure 6. Saturation magnetization on this plot is normally a line approaching a constant horizontal

slope; the asymptote projected to H = 0 defines the saturation magnetization, identical to the slope in Figure 5. Sample 11 was almost saturated when the experiment was terminated because of excessive horizontal displacement of the sample; ilmenites 12, 13 and 15 have similar and constant slopes above about 1500 Oe (12 x 10^4 A/m); sample 14 has a constant slope which passes through the origin indicating paramagnetic or antiferromagnetic behavior.

The steep sloped form of the curves 12, 13 and 15 is typical of materials at temperatures close to the Curie point (e.g., Bates, 1963, p. 310); it is also the characteristic of paramagnetic or antiferromagnetic materials which contain minor amounts of an additional ferri- or ferromagnetic phase (Cullity, 1972, p. 114). Saturation magnetization values ranges from zero for KK-ILM-14 to about 2 emu gm^{-1} (2 Am^2 kg^{-1}) for KK-ILM-11; samples 13 and 15 have identical saturation magnetization values (0.18 Am^2 kg^{-1}).

In the thermomagnetic curves (Figures 7a and 7b) reduced specific magnetization, $\sigma_T{}^0{}_k/\sigma_{296}{}^0{}_k$, is plotted against temperature. Field strengths indicated on the diagram are a compromise between convenient graphical display and a field strength compatible with observing the thermal decay of saturation magnetization. The reduced form of the magnetization obscures the field dependent magnetization differences between samples but allows analysis of the relative form of the curves.

There appear to be four types of behavior. Samples 1, 3 and 11 show Néel type Q or R curves (e.g., Standley, 1972, pp. 52-56) with well defined Curie points. Specimens 2, 4 and 14 display hyperbolic magnetization decay curves typical of paramagnetic substances following the Curie or Curie-

Weiss Laws (e.g., Mulay, 1963, p. 1764), or of the tail-end of a ferromagnetic curve. Ilmenites 12 and 13 behave intermediately to the above types. Sample 15 is relatively unusual in the linear form of its decay, which is typical of samples containing a range of solid-solution compositions and therefore a range of Curie temperatures; the apparent Néel type N behavior at about 550°c is probably an artifact of the record.

The σ/σ_0 values for the initially steep curves (e.g., samples 4 and 14) do not approach zero even above the hematite Néel point, suggesting that the Curie temperatures are low and that the induced paramagnetic moment existing above the transition temperatures are substantial relative to the total room temperature magnetization.

Figure 8a shows thermomagnetic curves for known hemoilmenite compositions. The σ/σ_0 values were calculated from absolute magnetization values of Nagata (1961, Fig. 3.31) and referenced to room temperature for the sake of comparison with our data. The forms of the curves for x = .47 and x = .67 are similar to the first and second types identified from Figure 7. Relative to more recent and reliable work (Readman and O'Reilly, 1972) the Curie temperature values of Nagata's ilmenites are not useful for comparison, although the relative form of the curves may be.

The shape of the thermomagnetic curve depends on applied field strength roughly as shown in Figure 8b (Nagata, 1961, Fig. 3.19). The Curie temperature does not change but is more easily identified in weak fields. Thermomagnetic curves for KK-ILM-1 to 15 are in various fields from 110 to 4000 Oe (8750 to 3.2 x 10^5 A/m), nevertheless the different forms of the curves are probably reflecting compositional differences in view of the different susceptibility and magnetization values (Figures 5

and 6).

To evaluate the preferred Curie temperature for KK-ILM-11 the Langevin-Weiss relation for ferromagnetic materials (e.g., Bates, 1963, pp. 275-280) is approximated by σ/σ_0 versus T/T_θ (Figure 9a). T_θ is the paramagnetic Curie temperature appearing also in the Curie-Weiss Law and is normally a few degrees higher than the ferromagnetic Curie temperature; for the correct value of T_θ the curve approaches T/T_θ as an inverse hyperbola. The majority of the magnetization of sample 11 has decayed by 320°c, but a higher temperature phase may exist to 340°c.

A method of estimating the Curie temperatures for the remaining samples is to plot reciprocal susceptibility versus temperature (see Figure 9b for KK-ILM-11); because susceptibility markedly decreases at the Curie or Néel temperature the extrapolation of the steep straight line segment of the plot to the temperature axis serves as an estimate of the Curie temperature (e.g., Zijlstra, 1967, p. 131). By this means (Figure 10) sample 14 shows a transition temperature at -50°c and samples 12 and 13 extrapolate to within $\pm$20°c of 200°c. The Curie point for KK-ILM-15 is probably within the range of 225 to 350°C.

If the compositions of these ilmenites are assumed to lie in the series $xFeTiO_3.(1-x)Fe_2O_3$ then according to the data of Readman and O'Reilly (1972) the measured Curie (Néel) temperatures correspond to compositions KK-ILM-11 x = 0.53; #15 x = 0.6 to 0.5; #'s 12 and 13 x = 0.6 to 0.62; and #14 x = 0.8.

Inclusion of other elements in place of iron lowers the Curie temperature, and for kimberlitic ilmenites it is well known (e.g., Haggerty, 1976) that the major substituent is magnesium, so that compositions more accur-

ately fall in the plane $FeTiO_3$-Fe_2O_3-$MgTiO_3$ (ilmenite-hematite-giekielite).

Compilations of compositional data for kimberlitic ilmenites from South and West Africa (Haggerty, 1976), and compositions and Curie points for Siberian kimberlitic ilmenites (Frantsesson, 1970) suggest, assuming each sample is single phase, the following compositions expressed as the ratio between $FeTiO_3$-Fe_2O_3-$MgTiO_3$: for KK-ILM-11 .53-.47-0; #14 6-1-4; #'s 12 and 13 7.5-2.5-2.5; and #15 6-4-1. The dilution of the compositions with magnesium would help to explain why the observed saturation magnetizations decrease with Curie temperature when the opposite behavior is observed in the central portion of the pure hematite-ilmenite system.

Reflected light oil-immersion microscopy of the samples from the thermomagnetic runs show that KK-ILM-14 is a single crystal of ilmenite; sample 11 is a highly altered polycrystalline ilmenite with exsolution lamellae of spinel. Sample #13 is also a highly altered ilmenite; volumetrically minor exsolution lamellae, probably of spinel, have been removed by alteration. KK-ILM-12 and 15 are ilmenites, optically similar to the host phase in sample 13; #15 is a highly strained crystal.

The magnetization curves, thermomagnetic runs and microscope observations can be reconciled as follows: Sample KK-ILM-14 is a single phase antiferromagnetic ilmenite; the magnetization curve is a straight line through the origin and the thermomagnetic curve is hypoerbolic with a subambient Néel point. The magnetization acquisition behavior and magnitude, and the thermomagnetic behavior (Néel type Q or R) of sample KK-ILM-11 are dominated by the exsolved spinel phase, most probably titano-magnetite.

The magnetic behavior of samples KK-ILM-12, 13 and 15 suggests that these specimens are not single phase, even although microscopic examination

did not resolve phases additional to the ilmenite. Inclusion of a submicroscopic ferrimagnetic phase would explain the form of the magnetization curves (e.g., Culltiy, 1972, p. 114), and also reconciles the intermediate thermomagnetic behavior of these samples. Additional evidence for this hypothesis is found in the lamellar pits of sample #13 (it is unlikely that all of the exsolved material has been totally removed) and in the Curie temperature-composition continuum shown by KK-ILM-15.

If, indeed, kimberlitic ilmenites frequently contain submicroscopic ferrimganetic inclusions, then deep-seated ilmenites may oe a potential source of lower crustal magnetization.

EXPERIMENTAL PROBLEMS

Initial problems in assembling the Curie Balance have been corrected by the manufacturers (Cahn-Ventron, Inc.) and our efforts. Cahn-Ventron has also recently supplied free of charge a replacement transformer to our own specifications so that the furnace is now capable of the manufacturer's specifications temperature (800°c).

We need to improve our temperature control, both in the high temperature system and in bringing the liquid Nitrogen cryostat to operational stage. Our continuing relationship with Cahn-Ventron has also suggested the possibility of our field testing new, more flexible temperature programmers under consideration by the company.

A combination of magnetic viscous effects at close to zero electromagnet voltage and zero applied field means that a dedicated Gaussmeter is required for weak ($\leq$ 550 Oe; $\leq$ .5 x 10^5 A/m) magnetic field experiments. A proposed purchase justification is attached as an Appendix. Presently

we are using a Gaussmeter on loan from the Physics Department at the University.

Poorly machined threads on one of the two electromagnet core retaining nuts allow the core to move in its mounting. The magnet manufacturer (Alpha Scientific) agreed that this is below tolerance and volunteered a free-of-charge repair if we incur shipping costs. We are loath to incur dead time for this relatively minor repair alone.

MAGSAT, GEOLOGICAL AND GRAVITY CORRELATIONS IN NORTHERN SOUTH AMERICA AND WEST AFRICA

We have examined the regional geology and geophysics of Northern South America and West Africa; data are assembled on the pre-drift fit of Bullard et al. (1965). The regional geology of fold belts, shield regions (Figure 11) and sedimentary basins (Figure 12) is compared to Bouguer gravity anomalies (Figure 13), radiometric dates (Figure 14), aeromagnetic data (Figure 15) and the north-south horizontal vector component (ΔX) of the Magsat anomaly field (Figure 16).

Gravity and Magsat data were graphically transferred from the referenced publications to the Bullard projection, but were not otherwise processed. Use of Bouguer gravity rather than Free Air values removes some of the effects of elevation and more accurately portrays continental subsea level information. The reassembled regions are presently at low geomagnetic latitudes and the horizontal component anomaly should fairly closely outline bodies with induced magnetization.

Sedimentary thicknesses in the Tauoudeni Basin of West Africa are roughly proportional to the geographically assocated Magsat positive (Hastings, 1982) and the Benue Trough has a positive signature (Frey, 1982). The Volta and Iullemedan Basins are also magnetically positive, although less distinctly (Figures 12 and 16).

A similar relationship is observed in South America (Hinze et al., 1982) and this is particularly evident in relation to the sediment isopachs for the Amazon, Parnaiba and Parana Basins (Figure 16). The Amazon Aulacogen is also a strong Bouguer positive (Longacre et al., 1982); in fact, most of the large positive Magsat anomalies within the reassembled area are spatially associated with positive Bouguer gravity anomalies and with gravity regions of short wavelength or low relief.

Project Magnet profiles (Figure 15) and aeromagnetic mpas (Strangway and Vogt, 1970; Behrendt and Watorson, 1974) show that long wavelength, low altitude magnetic anomalies become less intense from Liberian to Eburnean to Pan-African age rocks and generally follow the older structures. The trend is evident in Magsat maps for West Africa (e.g., Hastings, 1982; Figures 11, 14-16) but is less pronounced in South America, pernaps because the Jecquie-Guriense (Liberian) Age rocks are much less abundant (see Figure 11).

South American shield regions do not have a consistent relationsnip with Magsat and Free Air gravity anomalies (Hinze et al., 1982), but comparision with the Bouguer values in Figure 13 shows that shield regions in both South America and West Africa are characterized by negative Bouguer gravity anomalies. Thus the shields are loci for a density deficiency as well as a positive magnetic contrast. Tentative spatial correlations for

both shields and basins are listed in Table 1.

It seems that the striking coincidence of Magsat anomaly contours (Figure 16) achieved on reassembling this portion of Gondwanaland can be at least partially explained on the basis of the known geology. A coherent regional ge logic framework corresponds to the large scale geophysical features including Magsat anomalies. For the future, it would be useful to compare Magsat signatures with isostatic gravity anomalies calculated for different levels of compensation; the degree of internal correspondence between the two potential fields should help define whether the visual-spatial correlations noted here are due to the same sources, and at what depths within the crust.

SUMMARY

During the report period considerable progress has been made with the Curie Balance. The instrument can routinely measure room- and high-temperature magnetizations and has been successfully applied in the examination of a range of magnetic minerals.

Although there are persistent problems with the temperature and magnetic field control, analysis of a group of kimberlitic ilmenites from West Africa demonstrates that the instrument is capable of a high degree of resolution amongst relatively similar magnetic mineralogies.

Examination of MAGSAT anomaly maps for Northern South America and West Africa shows that the magnetic signatures can be coherently related to a regional geological and geophysical framework.

FUTURE WORK

We have accumulated a large backlog of samples for which tne mineral and geochemical data have already been acquired and the Curie Balance will be fully utilized in determining the magnetic properties of these materials. At tne same time we hope to improve the flexibility and utility of the instrument by bringing the temperature and tne magnetic field under tighter control.

We have noted some interesting geographical correlations between MAGSAT anomaly maps and parts of Africa and South America which are so encouraging close that we would like to put these comparisons on a more quantitative level. While this may be possible, the magnetic analytic and experimental work will have priority.

REFERENCES

de Almeida, F.F.M., Y. Hasui, B.B. de Brito Neves and R.A. Fuck (1981). Brazilian structural provinces: an introduction. Earth Science Reviews, 17, #1/2, 1-30.

Bates, L.F. (1963). Modern Magnetism. Cambridge University Press, London, 514 p.

Behrendt, J.C. and C.L. Wotorson (1974). Geophysical surveys of Liberia with tectonic and geologic interpretations. U.S.G.S. Prof. Pap. 810, 33 p.

Black, R. and M. Girod (1970). Late Paleozoic to Recent igneous activity in West Africa and its relationship to basement structure. In African Magmatism and Tectonics, edited by T.N. Clifford and I.G. Gass, pp. 185-210, Oliver and Boyd, Edinburgh, 461 p.

Bronner, G., J. Roussel, R. Trompette and N. Clauer (1980). Genesis and geodynamic evolution of the Taondeni Cratonic Basin (Upper Precambrian and Paleozoic), Western Africa. In Geodynamics of plate interiors, edited by A.W. Bally, P.L. Bender, T.R. McGetchin and R.I. Walcott, pp. 81-90, Geodynamics Series, Vol. 1, Amer. Geophys. Union, 162 p.

Bullard, E.C., J.E. Everett and A.G. Smith (1965). The fit of the continents around the Atlantic. Philos. Trans. Roy. Soc. London, A258, pp. 41-51.

Collinson, D.W., K.M. Creer and S.K. Runcorn (1967). Editors, Methods in Paleomagnetism, pp. 438-439, Developments in Solid Earth Geophysics, Vol. 3, Elsevier, N.Y., 609 p.

Cullity, B.D. (1972). Introduction to Magnetic Materials. Addison-Wesley Publ. Co., Reading, Massachusetts, 666 p.

Dillon, W.P. and J.M.A. Sougy (1974). Geology of West African and Canary and Cape Verde Islands. In The Ocean Basins and its Margins, Volume 2, The North Atlantic, edited by A.E.M. Nairn and F.G. Stehli, pp. 315-390, Plenum Press, N.Y., 598 p.

Earth Science Review (1981). Volume 17, #1-2, special issue on South America.

Frantsesson, E.V. (1970). The petrology of the kimberlites. Trans. D.A. Brown, Australian Natl. Univ. Publ. 150, 194 p.

Frey, H. (1982). MAGSAT scalar anomaly distribution: the global perspective. Geophys. Res. Lett., 9, 277-280.

Gunter, K.D. (1978). Correlation of paleomagnetic parameters with magnetic mineralogy in a detailed vertical traverse of the Holyoke Basalt, Holyoke, Massachusetts. Unpubl. M.Sc. Thesis (University of Massachusetts).

Haggerty, S.E. (1976). Opaque mineral oxides in temestrial rocks. In Oxide Minerals, short course notes, Vol. 3, edited by D. Rumble, pp. Hg 101-303, Mineralogical Society of America.

Hastings, D.A. (1982). Preliminary correlations of MAGSAT anomalies with tectonic features of Africa. Geophys. Res. Lett., 9, 303-306.

Hinze, W.J., R.R.B. von Frese, M.B. Longacre, L.W. Braile, E.G. Lidiak and G.R. Keller (1982). Regional magnetic and gravity anomalies of South America. Geophys. Res. Lett., 9, 314-317.

Hurley, P.M. and J.R. Rand (1973). Outline of Precambrian chronology in lands bordering the South Atlantic, exclusive of Brazil. In The Ocean Basins and Margins, Vol. 1, The South Atlantic, edited by A.E.M. Nairn and F.G. Stehli, pp. 391-410, Plenum Press, N.Y. 583 p.

Langel, R.A.. C.C. Schnetzler, J.D. Phillips and R.J. Horner (1982). Initial vector magnetic anomaly maps from MAGSAT. Geophys. Res. Lett., 9, 273-278.

Lindoy, L.F., V. Katovic and D.H. Busch (1972). A variable temperature Faraday magnetic balance. J. Chem. Ed., 49, 117-120.

Longacre, M.B., W.J. Hinze and R.R.B. von Frese (1982). A satellite model of Northeastern South American Aulacogens. Geophys. Res. Lett. 9, 318-321.

Morris, B.L. and A. Wold (1965). Faraday balance for measuring magnetic susceptibility. Rev. Sci. Instrum., 39, 1937-1941.

Mulay, L.N. (1963). Magnetic Susceptibility. John Wiley and Sons, Inc., N.Y., 132 p.

Müller, M. and H.J. Güntherodt (1981). A pendulum balance for high temperature magnetic susceptibility measurements. J. Phys. E. Sci. Inst., 14, 453-456.

Nagata, T. (1961). Rock Magnetism. Maruzen Company, Ltd., Tokyo, Japan, 350 p.

Nairn, A.E.M. and F.G. Stehli (1973). The Ocean Basins and its Margins, Vol. 1, The South Atlantic, edited by A.E.M. Nairn and F.G. Stehli, Chapters 2, 10, 11 and 12, Plenum Press, N.Y. 583 p.

Radhakrishnamurthy, C. and S.D. Likhite (1970). Hopkinson effect, blocking temperature and Curie point in basalts. Earth and Planet. Sci. Lett., 7, 389-396.

Readman, N.I. and W. O'Reilly (1972). Magnetic properties of oxidised (cation-deficient) titanomagnetites $(Fe, Ti)_3O_4$. J. Geomag. and Geoelect., 24, 69-90.

Schwarz, E.J. (1968). A recording thermomagnetic balance. Geol. Surv. Canada, Paper 68-37, 11 p.

Schwarz, E.J. (1974). Magnetic properties of pyrrhotite and their use in applied geology and geophysics. Geol. Surv. Canada, Paper 74-57, 24 p.

Slettene, R.L., L.E. Wilcox, R.S. Blouse and J.R. Saunders (1973). A Bougeur gravity anomaly map of Africa, 1:20 million. Tech. Pap. 73-3, Offices of Distribution Services, U.S. Defense Mapping Agency, Washington, D.C.

Standley, K.J. (1972). Oxide magnetic materials. Clarendon Oxford University Press, London, 254 p.

Strangway, D.W. and P.R. Vogt (1970). Aeromagnetic tests for continental drift in Africa and South America. Earth and Planet. Sci. lett., 7, 429-435.

Wilcox, L. (1976). Automated Library System and Services of DMA (Regional Gravity and Elevation Maps of South America). In Geophysics in the Americas, edited by J.G. Tanner and M.R. Dence, pp. 114-117 (maps in sleeve), Earth Physics Branch publication Vol. 46 #3, Energy, Mines and Resources, Ottawa, Canada, 259 p.

Zijlstra, H. (1967). Experimental Methods in Magnetism. 2. Measurement of Magnetic Quantities. Solid State Physics Monographs, volume 9, series editor E.P. Wohlfarth, John Wiley and Sons, Inc., N.Y., 296 p.

FIGURE CAPTIONS

Figure 1. Magnetic field characteristics of the Curie Balance electromagnet with respect to the vertical axis, at a one inch pole gap and 25 amps (1 kOe = 7.96 x 10^4 A/m; 1kOe/cm = 6.34 x 10^{11} A^2/m^3). The sample location in the region of constant HdH/dz is indicated.

Figure 2. Magnetization curves for the Holyoke Basalt. The upper curve was measured at Bell Laboratories; the lower curve from our Curie Balance is encouragingly close in value.

Figure 3. Thermomagnetic curve for the Holyoke Basalt. The y-axis is magnetic intensity transduced as milligrams and the x-axis is tnermocouple millivoltage. Temperature is calibrated for the heating cycle, which shows for this sample a steady loss of magnetization with temperature and a single well defined Curie point of about 575°c. The cooling cycle is at an uncontrolled rate. The weight change over the whole cycle is probably due to devolatilization.

Figure 4a. Thermomagnetic curve for a magnetically unknown sulphide sample.

Figure 4b. Thermomagnetic curve for a sample containing Fe_7S_8 and Fe_9S_{10} (Schwarz, 1974). Comparison with Figure 4a suggests that our unknown sample contains both these magnetic phases.

Figure 5. Specific susceptibility versus reciprocal field strength for kimberlitic ilmenites KK-ILM-11 to 15. Sample 14 is antiferromagnetic or paramagnetic; samples 12, 13 and 15 display ferro- or ferrimagnetic form but with very low susceptibilities. Ilmenite 11 is more strongly magnetic and is plotted on a reduced ($\times 10^{-1}$) scale.

Figure 6. Specific magnetization versus field strength for kimberlitic ilmenites. Sample 11 was close to saturation magnetization when the experiment was terminated. Specimens 12, 13 and 15 have magnetization curves typical of materials close to tne Curie point or of weak magnetic materials which include a minor ferro- or ferrimagnetic second phase. Sample KK-ILM-14 has a curve of constant slope (susceptibility) passing through the origin.

Figures 7a and 7b. Thermomagnetic curves for kimberlitic ilmenites KK-ILM-1 to 4 and 11 to 15. The thermomagnetic curves are plotted as σ/σ_0 versus temperature, allowing comparison of the relative forms of the decay magnetization. Samples 1, 3 and 11 display marked Curie points (333°c, 455°c and 340°c), whereas the other curves mostly follow a hyperbolic Curie Law.

Figure 8a. Thermomagnetic curves for selected hemoilmenite compositions (from Nagata, 1961). Comparison of the figure with Figure 7 suggests that the envelope of curves for the kimberlitic ilmenites corresponds to a chemical compositional range.

Figure 8b. Thermomagnetic curves for a titano-magnetite in various field strengths (from Nagata, 1961). The form of the thermomagnetic curve changes with field strength, thus qualifying the comparisons between Figure 8a and Figure 7.

Figure 9a. Reduced thermomagnetic curve for KK-ILM-11. T_Θ is the nominated Curie temperature and T_Θ = 320°c appears graphically to be the best fit.

Figure 9b. Reciprocal susceptibility versus temperature for KK-ILM-11. On this diagram the Curie point is found to be 317°c.

Figure 10. Reciprocal susceptibility versus temperature for KK-ILM-11 to 15. Transition temperatures derived from the figure are

KK-ILM-11 320°c
12 225°c
13 190°c
14 -50°c
15 200-350°c

Figure 11. Regional geologic structure of Northern South America and West Africa. The map is compiled from Nairn and Stehli (1973); Earth Science Review, volume 17, 1-2 (1981); Black and Girod (1970); Dillon and Sougy (1974); and Bronner et al. (1980), on the base map from Bullard et al. (1965); present geographic coordinates are indicated. The map snows the regional framework of cratons divided into shields and basins, separ-

ated by fold belts or sutures.

Figure 12. Sedimentary basins and sediment isopachs for Northern South America and West Africa. Main references are Bronner et al. (1980); de Almeida et al. (1981); see also Wilcox (1977) and Black and Girod (1970). Sediment thicknesses are in kilometers.

Figure 13. Bouguer gravity anomalies for Northern South America and West Africa. Data for South America are from Wilcox (1977) and for West Africa from Slettene et al. (1973). Contours are in milligals; the contour level is not constant. The gravity anomalies are closely related to the regional geologic structure as shown by comparison with Figures 11 and 12.

Figure 14. Schematic representation of Precambrian age provinces in Northern South America and Southern West Africa. The figure is from Hurley and Rand (1974). Shield areas are divided according to the age of the last dominant orogeny, either 2000 or 2700 my. Mobile belt ages are more widely scattered, but congregate at about 600 my.

Figure 15. Project Magnet aeromagnetic profiles over Northern South America and Southern West Africa (Strangway and Vogt, 1970). Long wavelength aeromagnetic anomalies become less intense over more recently tectonized rocks (see also Behrendt and Wotorson, 1974).

Figure 16. MAGSAT ΔX anomalies for Northern South American and West Africa. Taken from a map equivalent to Fig. 1 of Langel et al. (1982).

ΔX is the north-south horizontal component of the MAGSAT anomaly, selected for comparison because the Earth's inducing field is close to horizontal at the present latitudes. The major features of the map can be closely related to the regional geology and geophysics of the area.

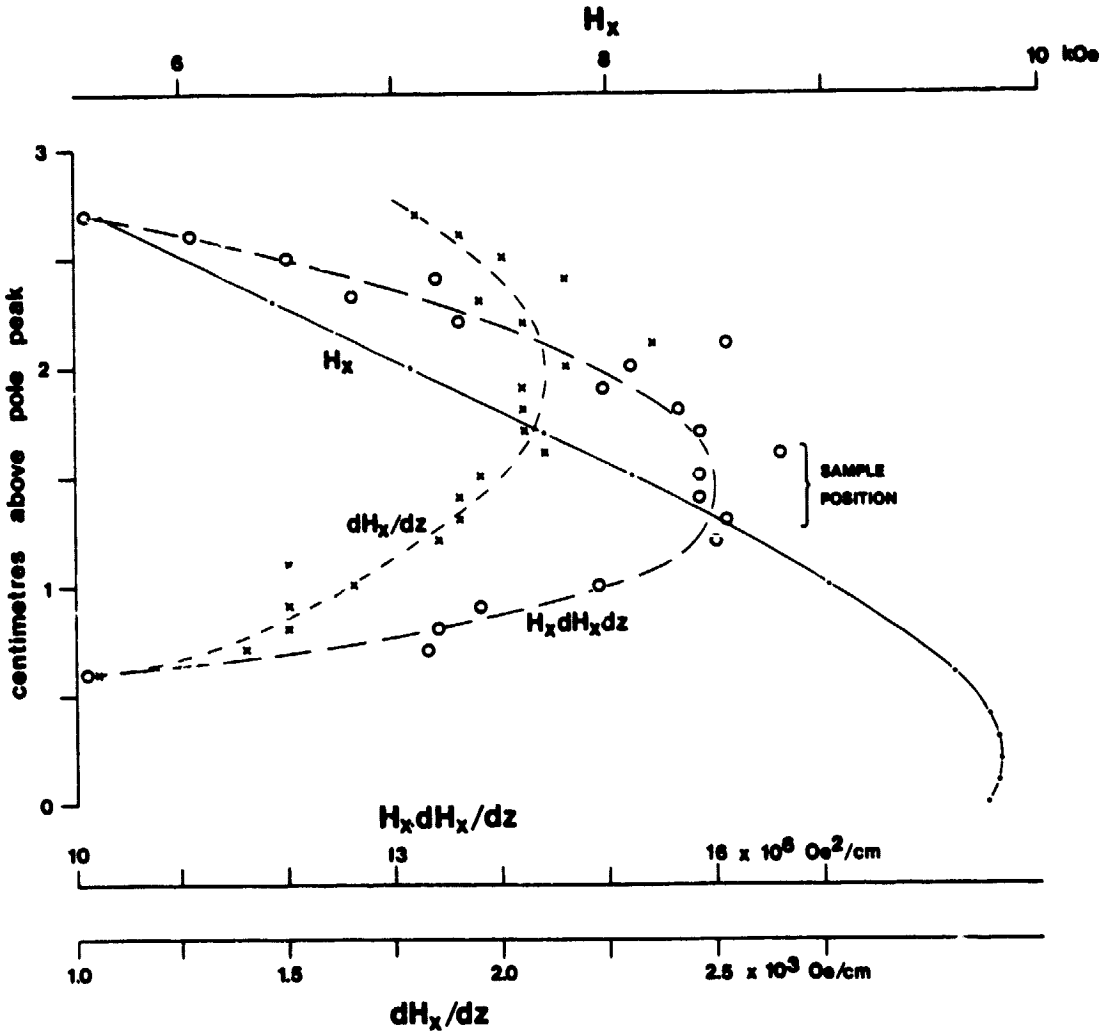

Figure 1

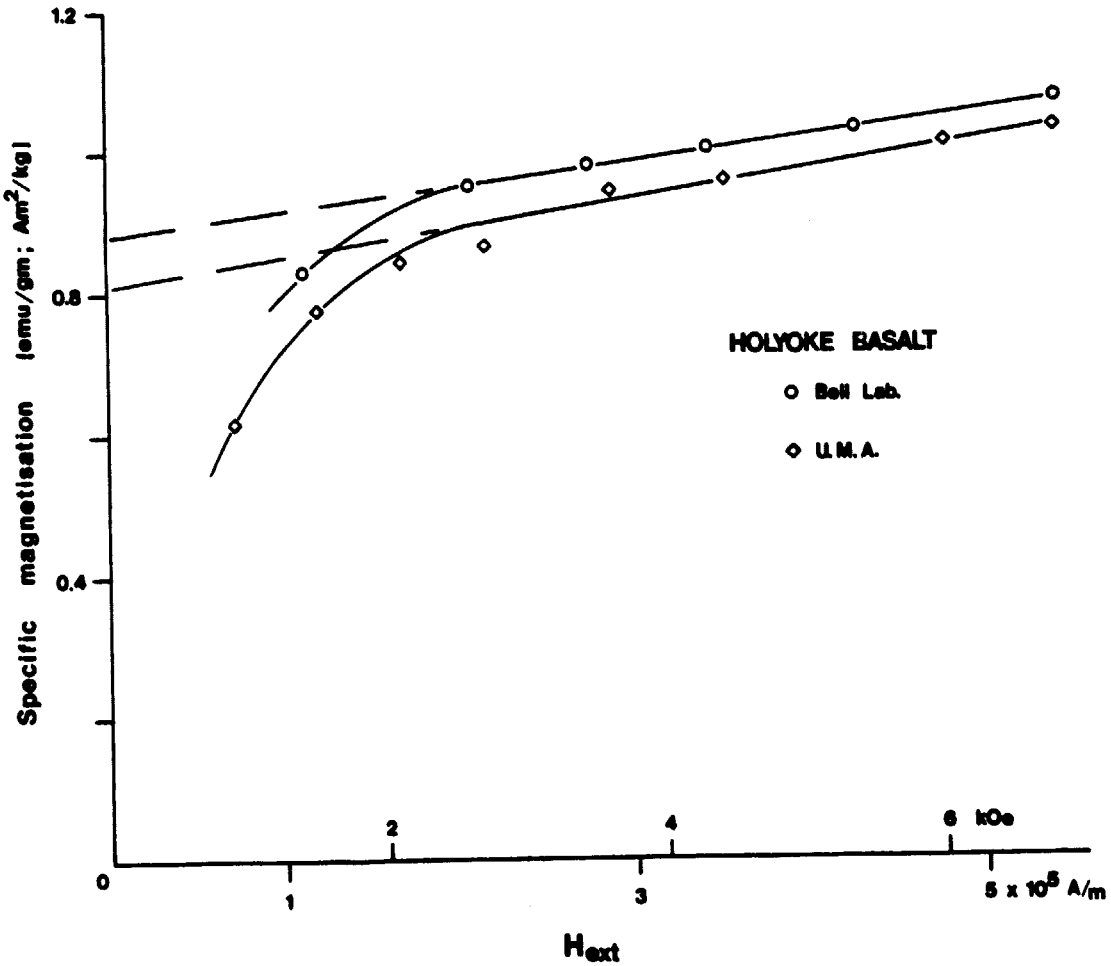

Figure 2

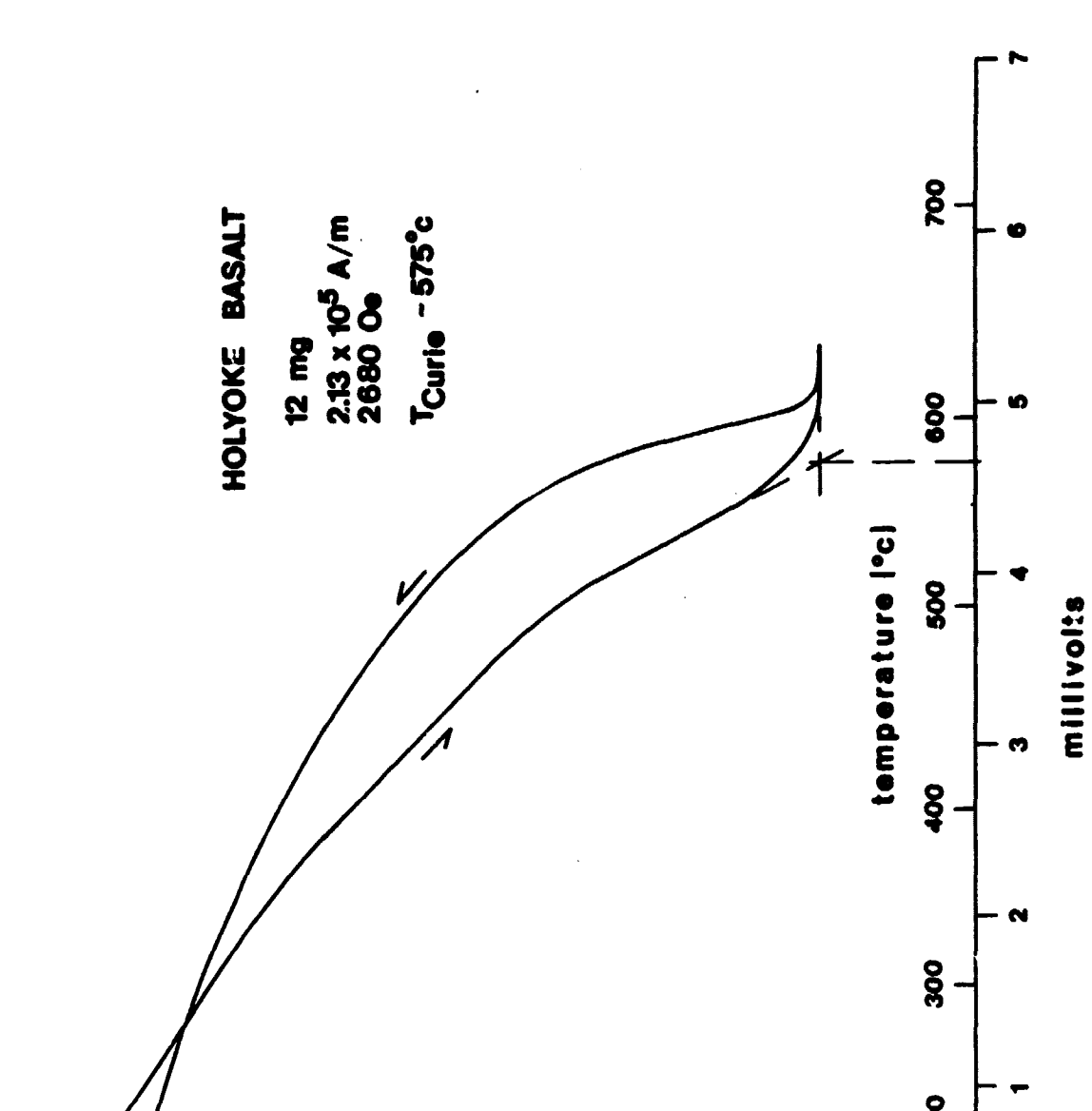

Figure 3

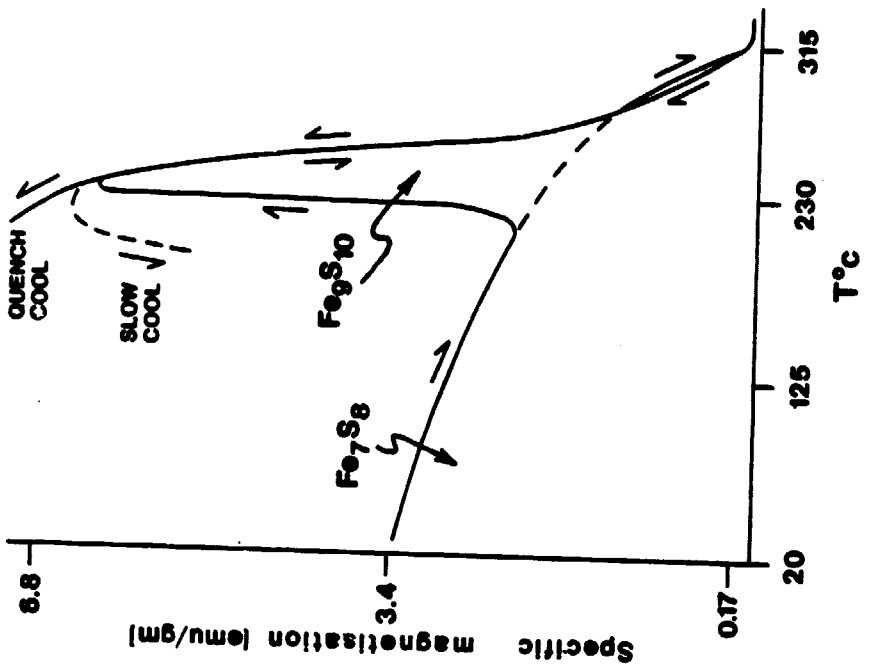

Figure 4b

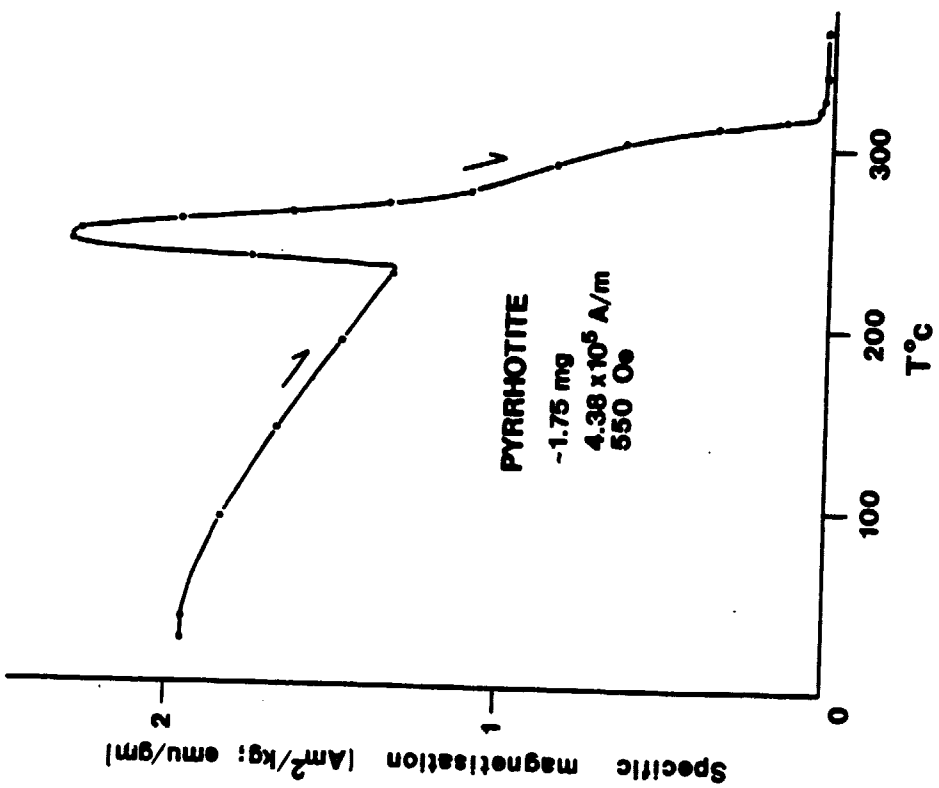

Figure 4a

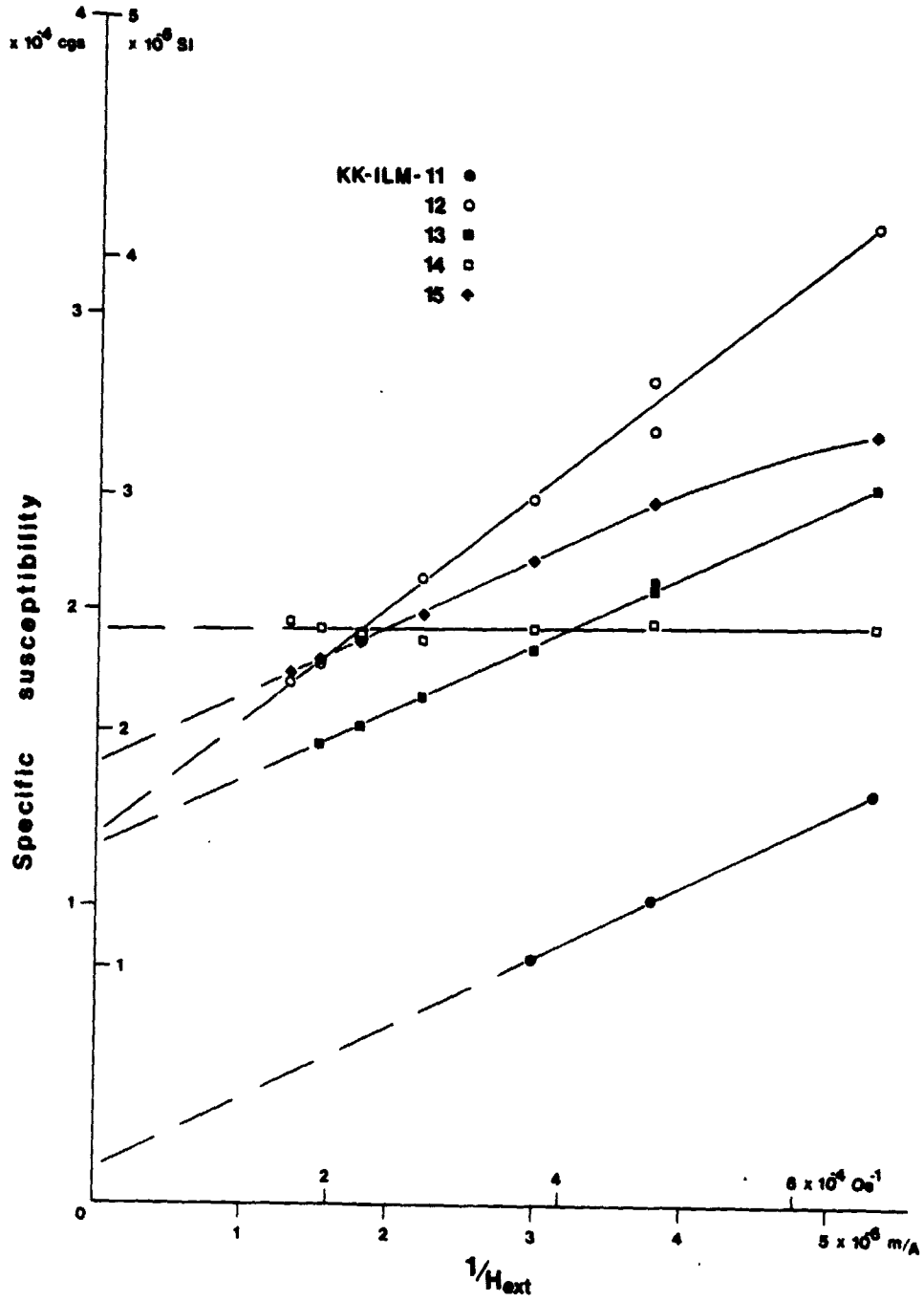

Figure 5

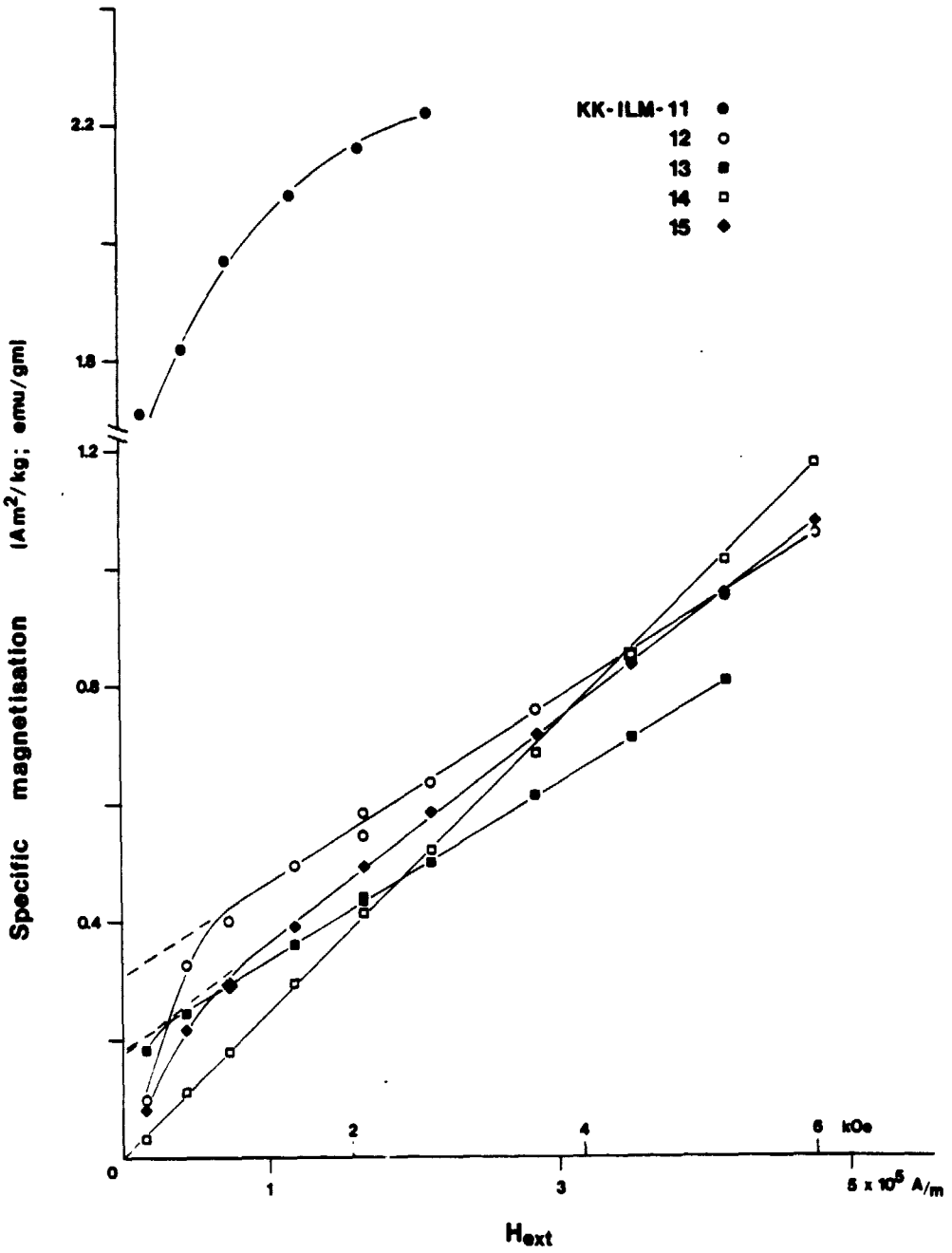

Figure 6

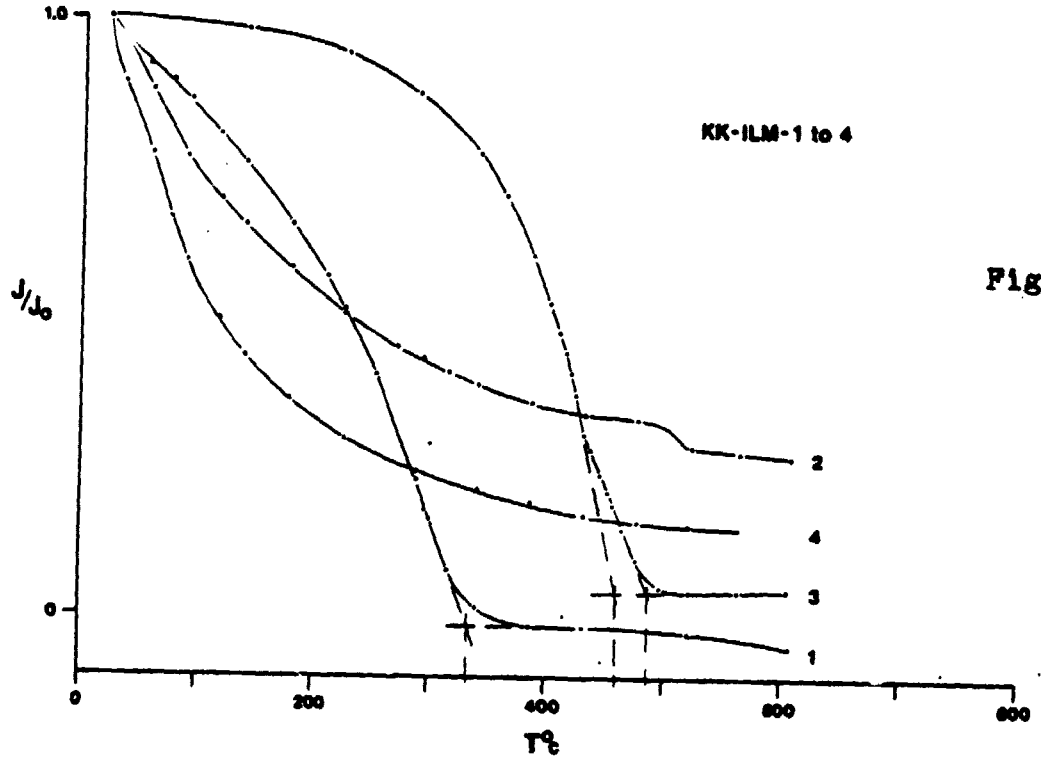

Figure 7a

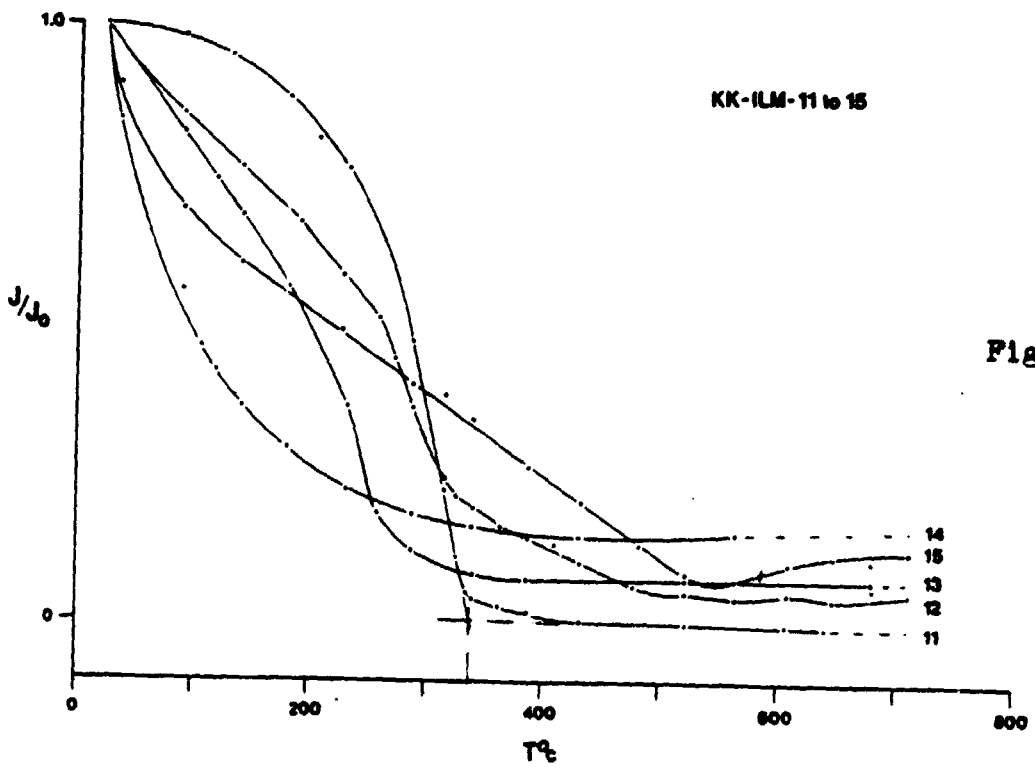

Figure 7b

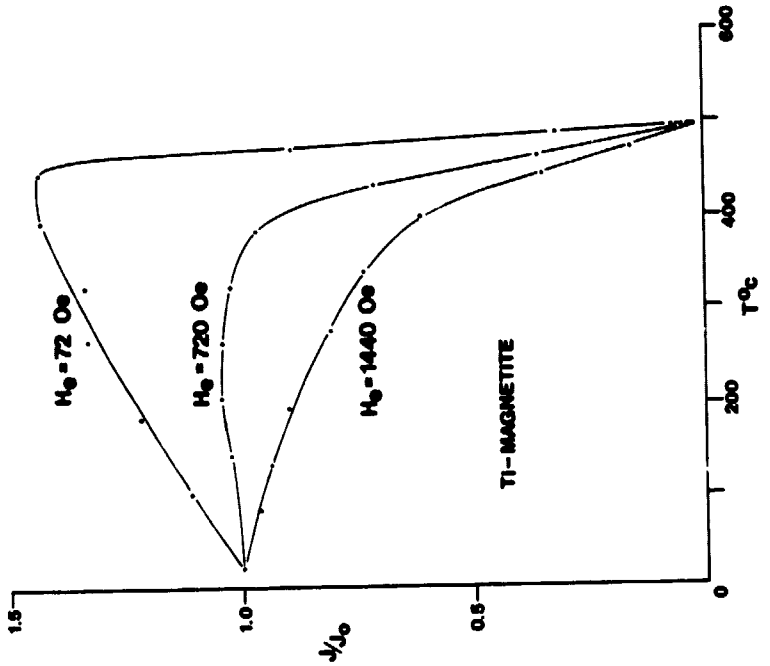

Figure 8b

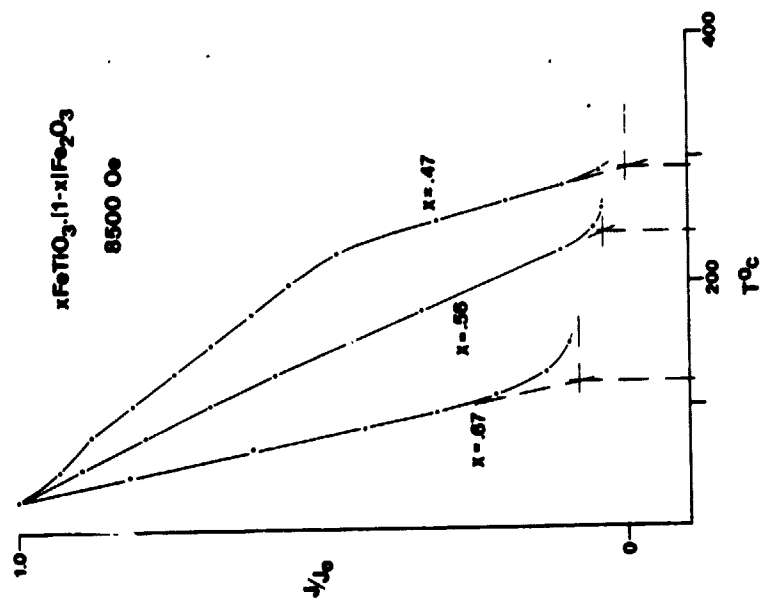

Figure 8a

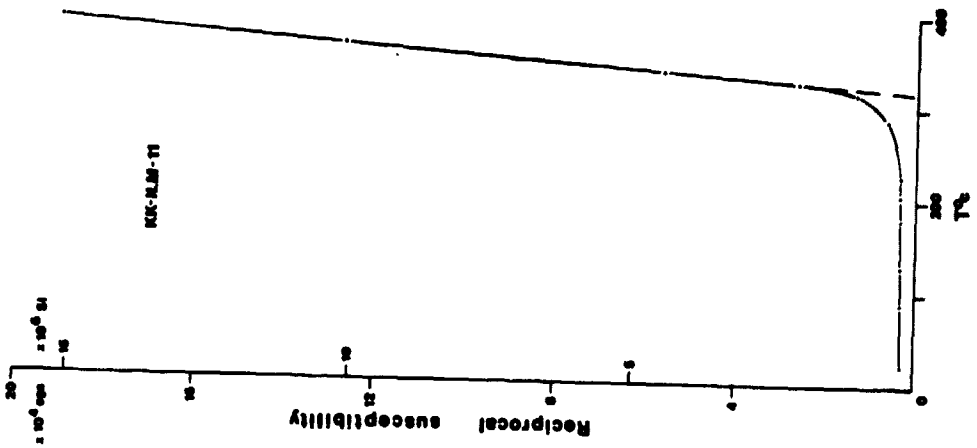

Figure 9b

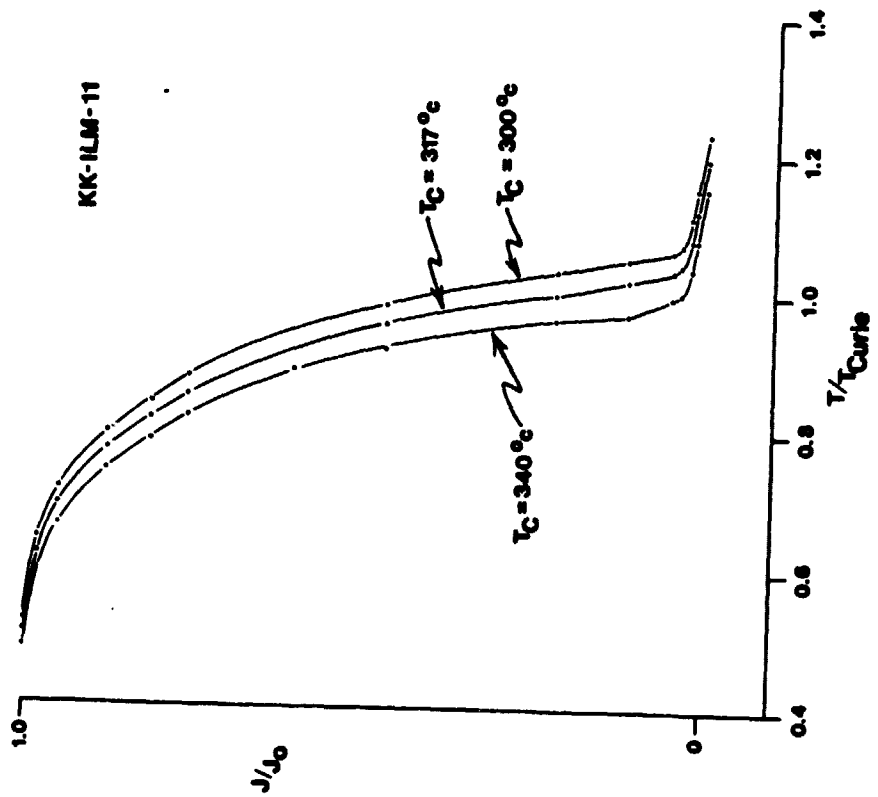

Figure 9a

ORIGINAL PAGE IS
OF POOR QUALITY

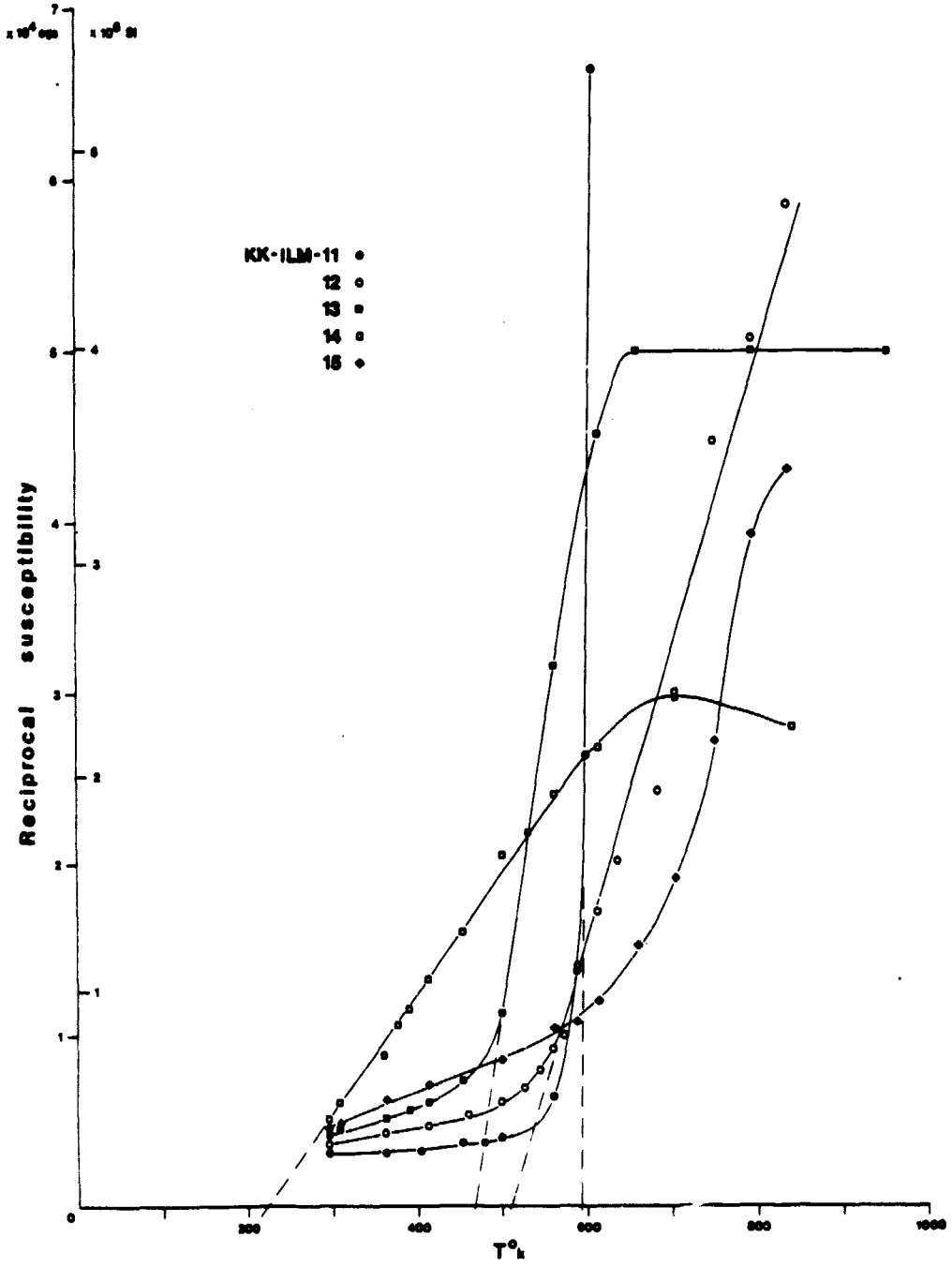

Figure 10

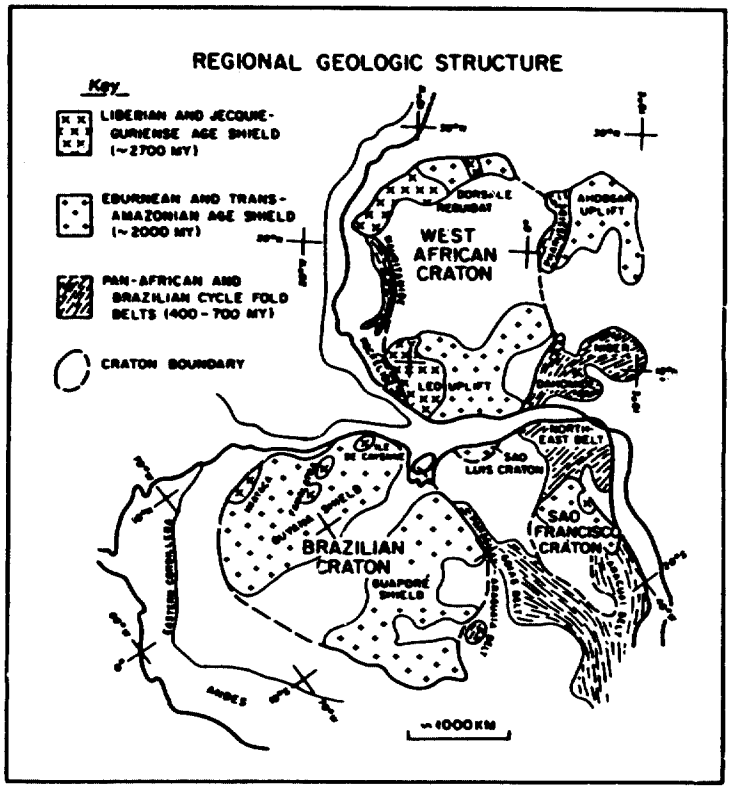

Figure 11

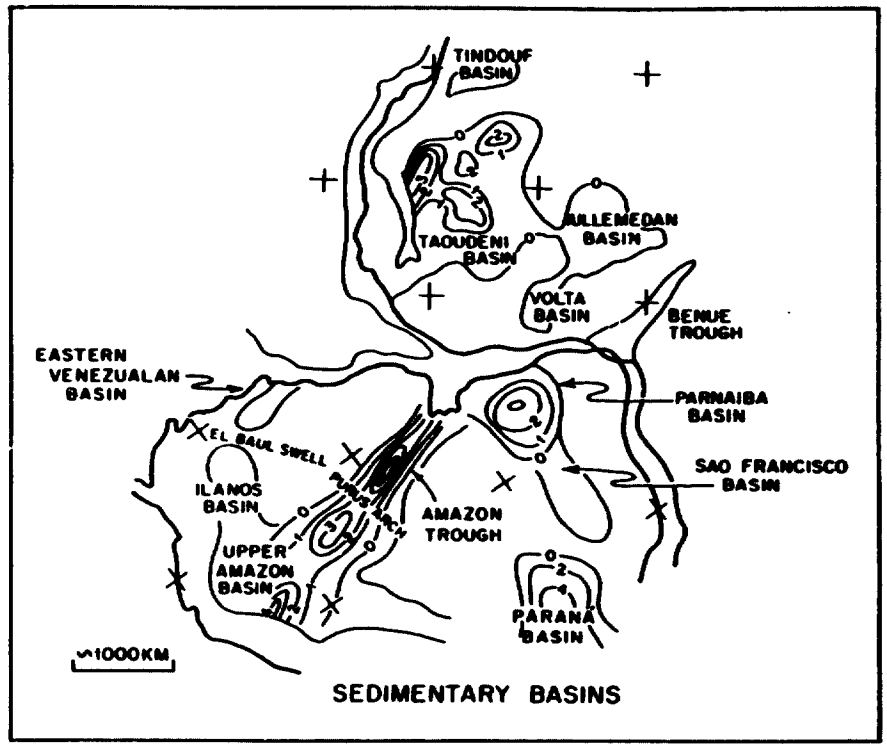

Figure 12

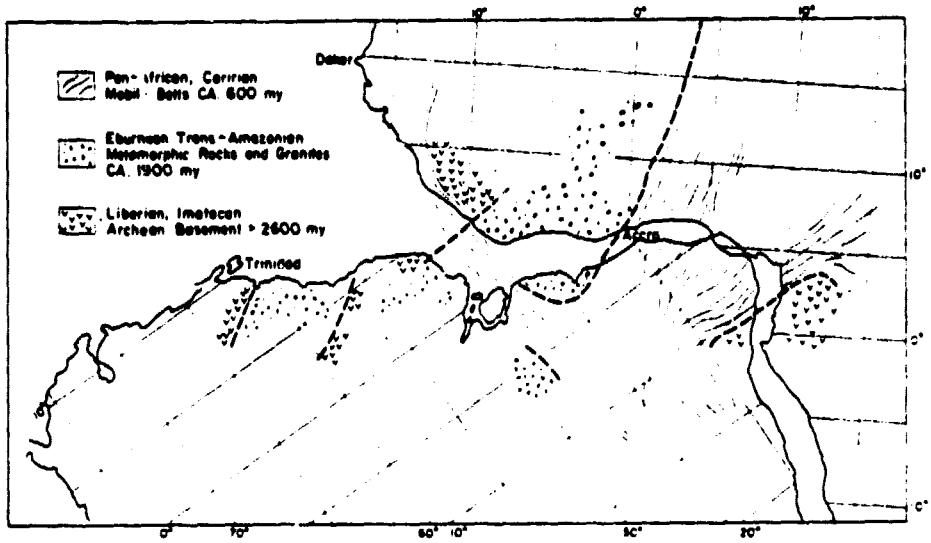

Fig. 14 Schematic representation of Precambrian age provinces (Hurley and Rand, 1974, figure 5)

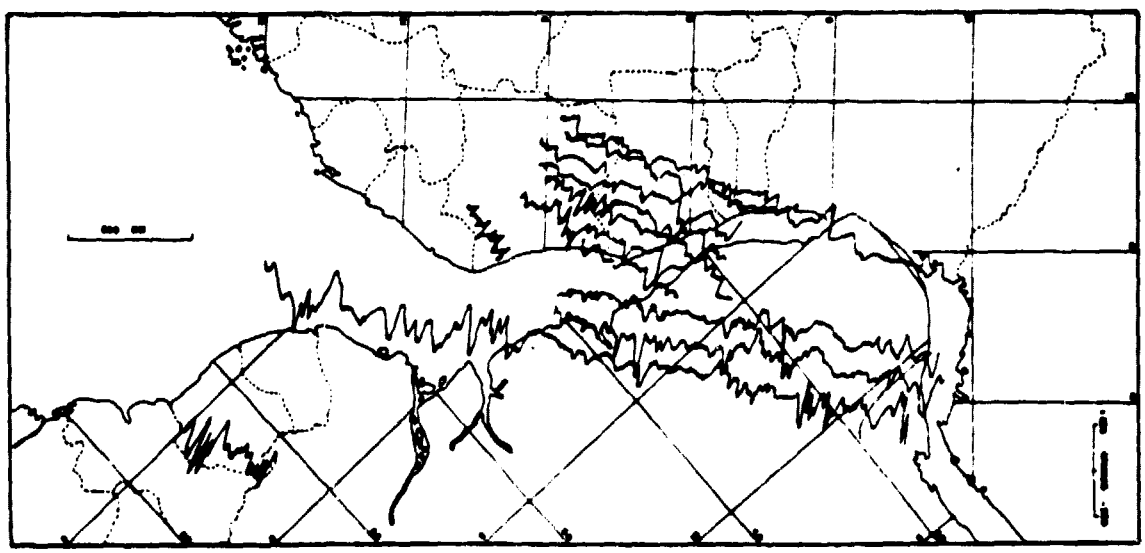

Fig. 15 Project Magnet aeromagnetic profiles (Strangway and Vogt, 1970, figure 4)

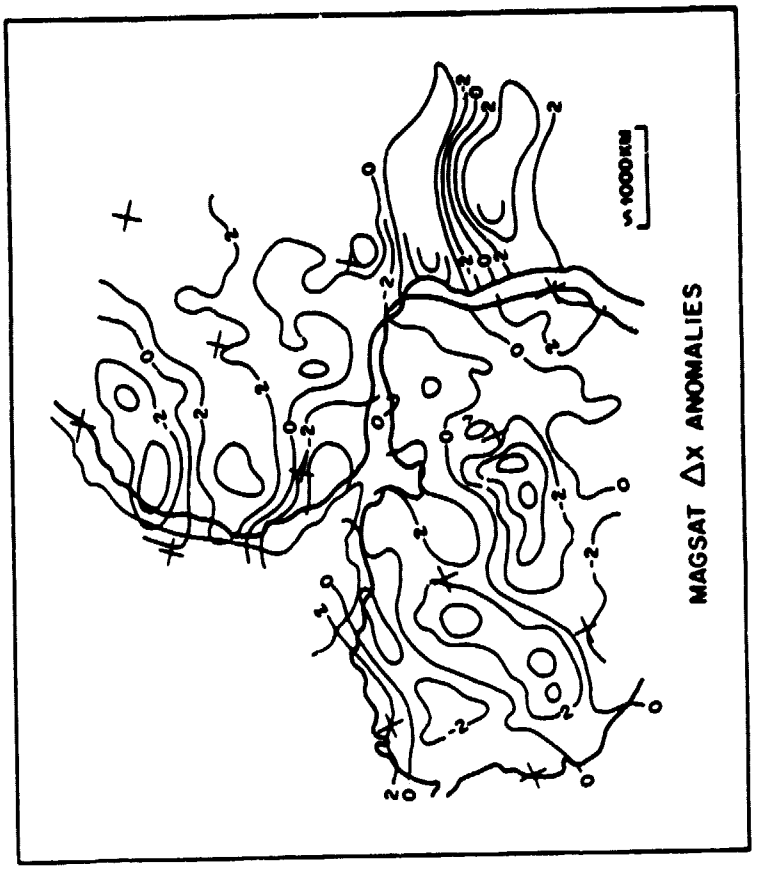

Figure 16

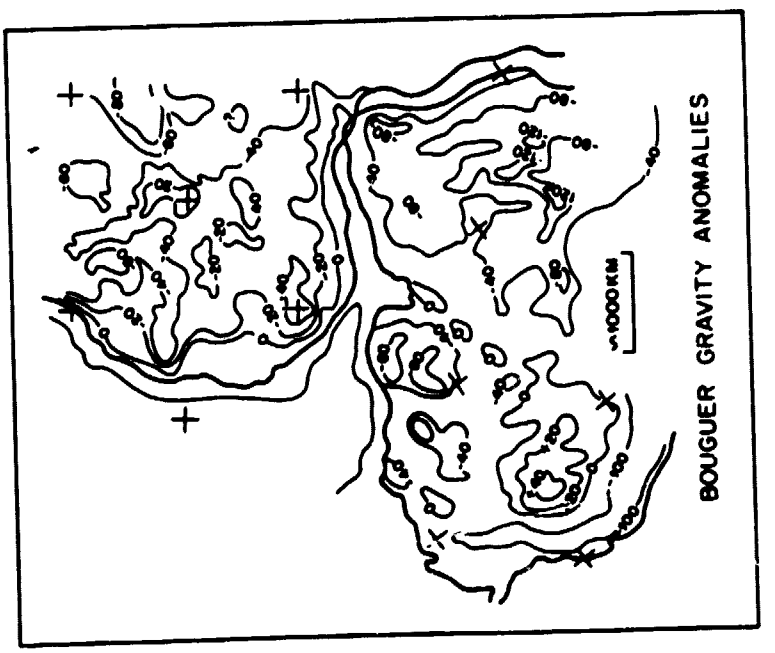

Figure 13

CORRELATIONS OF BOUGUER GRAVITY AND REGIONAL GEOLOGY WITH MAJOR FEATURES OF THE MAGSAT ΔX ANOMALIES OF NORTHERN SOUTH AMERICA AND WEST AFRICA

NOMINAL NAME	MAGNETIC SIGNATURE	GRAVITY SIGNATURE	GEOLOGICAL ASSOCIATIONS
South America			
Imataca	-2 nT	-10 to -20 mgal	Imataca Complex and Sarama Mazaruni Asemblage of the northern Guyana Shield
El Baul	locally + break in -2 nT	-10 to -30 mgal, on gradient between + and - peaks	El Baul Swell
Columbia	-2 nT	0 to -100 mgal, an area of low gravity relief, flanking low to the west	Ilanos Basin and Eastern Cordillera of the northern Andes
Eastern Amazon Basin	+2 nT	an area of short (2°) wavelength anomalies, +30 to -50 mgal	deepest part of the Amazon Basin, locally 4 km of sediments
Upper Amazon Basin	+4 nT	0 to +30 mgal, on flank of largest Bouguer + in South America	Upper Amazon Basin, on Arch between 4 km sediments to west and 3 km to east
Middle Amazon	+4 nT	an area of low relief, a relatively positive feature, +10 to -30 mgal	southern margin of Guyana Shield, on strike with Purus Arch and El Baul Swell
Parnaiba Basin	+2 nT (?)	-80 mgal	centered over maximum thickness of Parnaiba Basin sediments (3 km) and 400 m of intrusive diabases
Guaporé Shield	-6 nT	0 to -60 mgal	Trans-Amazonian age (?) Guaporé Shield
Goias	?	-30 mgal, locally positive feature within regionally negative Bouguer values	Paraguay-Araguaia Brazilian Cycle fold belt
Minas Gerais	+2 nT	on steep coastal gradient of Bouguer; area of short (3°) wavelength Free Air anomalies, ±30 mgal	possible extension of the southern positive of the Bangui anomaly; Araçuai Fold Belt; (includes region of Vargem kimberlite)
West Africa			
Western Reguibat	-4 nT	0 to -50 mgal	northern Mauritanides Fold Belt; Liberian age equivalent rocks of the Dorsale Reguibat
Central Reguibat	locally + break in -4 nT contour	local + (-20 to -40 mgal) on regionally - Bouguer values	Eburnean age equivalent granitic rocks of the Dorsale Reguibat
Eastern Reguibat	-4 nT	-40 to -60 mgal	Liberian age equivalent rocks of the Dorsale Reguibat; Tindouf Basin
Taoudeni	+4 nT	0 to -20 mgal, local positive embayment in negative Bouguer contours	Southern Mauritanides; locally thin (< 1 km) sediments of the Taoudeni Basin
Leo Uplift	-4 nT	0 to -40 mgal	< - 4 nT: Rockelide fold belt, Liberian province of the Leo Uplift < - 4 nT: also includes the Eburnean age province
Volta	+2 nT	-20 to -30 mgal, locally positive embayment in gravity contours	Volta-Buem-Togo formations of the Volta Basin
Niger	> -2 nT	-40 to -60 mgal (?)	Iullemedan Basin
Ahoggar	+2 nT	-80 mgal	Ahoggar Uplift

APPENDIX

PROPOSED PURCHASE OF GAUSSMETER

JUSTIFICATION

A Gaussmeter is essential to the operation of the Cahn Curie Balance Magnetic Susceptibility System because the magnetic parameters measured depend upon magnetic field strength. The relationship of field strength to the electromagnet voltage or current is presently calibrated and monitored by a Gaussmeter on temporary loan from the Physics Department at the University of Massachusetts. Due to magnetic viscosity of the pole caps, the field strength-voltage relationship at low intensity fields is not repeatable, and successful operation of the system therefore requires a dedicated Gaussmeter.

EVALUATION OF GAUSSMETERS

The optimum and cheapest method for measuring magnetic fields in the Curie Balance is based on the Hall effect sensor. The sensor unit alone is available from Walker Scientific (W.SI. I-1-10k; $138.00). However, this option would require in-house construction of a stabilized 100 mA power supply and a dedicated voltmeter with 0.01 mV resolution.

Market research of domestic U.S. companies which manufacture complete and suitable Gaussmeters (F.W. Bell, Inc.; RFL industries, Inc.; Walker Scientific, Inc.; Magnetic Instrumentation, Inc.; LDJ Electronics, Inc.) is broken down and evaluated as follows (see attached literature).

In the price range below $900.00 the RFL model 904 is superior in the

method of calibration and in accuracy, and in low field resolution (to ±1 Gauss); it is also available in S.I. units.

In the range $900.00 to $1200.00 the Walker model MG5D is superior. The advantages over the RFL model 904 are an increased resolution (to ±0.1 Gauss) and accuracy, and the digital readout. Gaussmeters in the price range $1200.00 to $1550.00 are included for comparison; the Magnetics Instrumentation model 7305 is superior and the Walker model MG2A is equivalent to the meter now on loan to us from the Physics Department.

CONCLUSION

From this market research the cheapest and most suitable Gaussmeter believed to be available is manufactured by RFL Industries, Inc. The complete unit for the RFL model 904 is broken down as:

RFL Gaussmeter 904	$420.00
RFL Hall probe 904 039	185.00
RFL zero-Gauss reference chamber HA-16580	40.00
	$645.00

Purchase of the RFL 904 Gaussmeter would greatly facilitate our magnetic experimental work at a relatively minor cost.

$420.00

MODEL 904 GAUSSMETER
MODEL 904T TESLAMETER

RFL

Wide-Range Measurement - 1.0 Gauss to 30 Kilogauss (0.0001 to 3 Tesla)

Automatic Field-polarity Indicator

Built-In Electronic Calibration System

Pushbutton Range Selection

Bipolar Analog Indicator for Ease of Operation

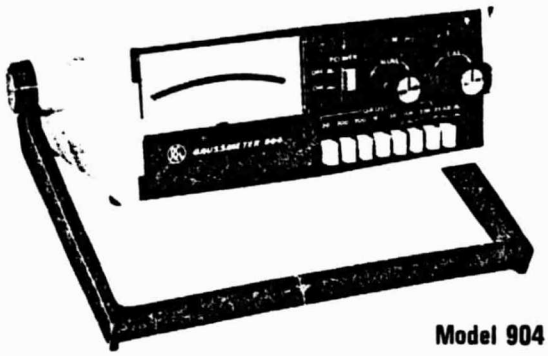

Model 904

The Model 904 is a compact instrument designed for measuring intensity of ac, dc, and permanent-magnet magnetic fields with flux densities from 1.0 to 30,000 gauss (0.0001 to 3 Tesla). The Model 904 Gaussmeter reads flux density in gauss. The Model 904T Teslameter reads flux density in tesla. The two models are identical in all other respects. A wide choice of Hall-effect probes is available to enable the meter to measure many different configurations of both transverse and axial magnetic fields. Each probe is marked with its own calibration factor, measured at the factory, to facilitate use of the accurate, internal calibration circuit.

Flux density is read from a parallax-corrected, analog meter with a three-inch scale. An automatic bipolar circuit gives this indicator the resolution and scale length of a zero-center, six-inch bipolar meter. All fields, irrespective of polarity, use the zero-left scale, and North or South polarity is indicated by illumination of an appropriately marked light-emitting diode.

The span of measurement is covered in seven full-scale ranges with scaling factors of 1 and 3. Static (dc and permanent-magnet) fields are read directly from the front-panel meter. For dynamic (ac) fields, an analog output with a range of ±1.0 volt for any full-scale range enables fields from 10 to 1000 Hz to be measured. A sensitive ac voltmeter or an oscilloscope are usually used. The analog output also facilitates use with an external recorder, or it may be used as a control signal for automatic or semiautomatic magnetic-processing systems.

The Model 904 is packaged in an impact-resistant plastic enclosure, and it is equipped with a carrying handle that serves also as a tilt-bail support for ease of operation and viewing.

SPECIFICATIONS

Full-scale Ranges: Model 904 Gaussmeter: 0 to 30, 100, 300, 1K, 3K, 10K, 30K Gauss.

Model 904T Teslameter: 0 to 0.003, 0.01, 0.03, 0.1, 0.3, 1.0, and 3.0 Tesla.

Accuracy: For permanent-magnet, dc, and ac fields from 10 to 400 Hz: ±(3% of range plus error of probe).

For ac fields from 401 to 1000 Hz: ±(5% of range plus error of probe).

Downscale Linearity: ±1% of range.

Operating Temperature Range: 12°C to 32°C.

Calibration Method: Built-in electronic circuit calibrated against 0.2% magnetic reference standard.

Analog Output: ±1 volt full-scale for any range.

Range Selection: Pushbuttons.

Operating Power: 115/230 Vac, 48-63 Hz, approx. 3.5 watts.

Size: 8.25" wide, 9" deep, 2.75" high (209 x 228 x 70 mm).

Weight: 3.8 lbs., (1.7 kg.)

Hall Probes for use with Models 904 and 904T: See page 46.

Resolution 0-30 Gauss - 1 Gauss division 1.0
0-10 KGauss - 200 Gauss division 200

RFL Industries, Inc.
Boonton, New Jersey U.S.A.

WALKER SCIENTIFIC INC.

MG-5D
Portable Laboratory Gaussmeter

GENERAL:

The MG-5D is a general purpose portable Hall effect gaussmeter designed to measure both DC & AC (RMS) magnetic fields.

Three full-scale bipolar ranges of ±100.0 gauss, ±1,000 gauss and ±10.00 KG with 100% over-range and resolution of 0.05% provides DC & AC field readings from ±100 milligauss to ±19.99 KG with true RMS readings from 5 Hz to 20 KHz; readings are displayed on a 3½ digit ±0.05% bipolar LCD meter.

A wide selection of precalibrated transverse and axial Hall probes are available to meet most every application, including probes which will extend the measuring range of this instrument to 150.0 KG.

The MG-5D operates either from AC or from four standard "D" cell alkaline batteries. During AC operation, the batteries receive a trickle charge which keeps them fresh until the instrument is required for portable use. Freshly charged batteries will continuously operate this instrument for approximately 50 hours.

In addition, an analog output is also provided for external monitoring.

APPLICATIONS:

- Measure Residual Fields
- Analyze Magnetic Circuits and Components
- Classify Magnets
- Measure Absolute & Differential Fields
- Plot Field Uniformity
- Measure Stray & Leakage Fields

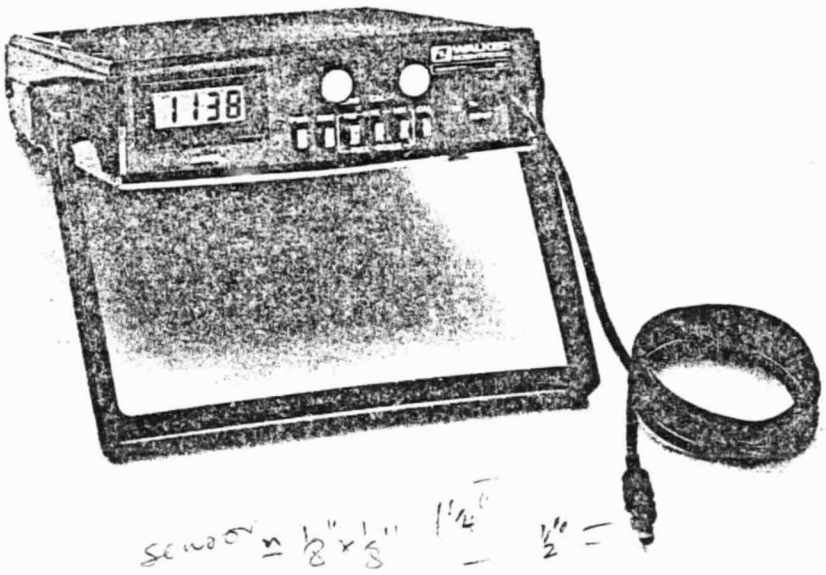

FEATURES:

- 3½ Digit ±0.05% Bipolar Display
- DC & AC Fields, ±100 milligauss to ±19.99 KG with 1X probes
- Range Extendable to 150.0 KG with Select Probes
- True RMS Readings to 20 KHz
- Wide Selection of Precalibrated Probes: 1X, 10X & 100X
- Operates with either AC or Battery; Fully Portable
- Analog Output; For External Monitoring
- High Impact Plastic Case with Carrying Handle
- One Year Warranty

ACCESSORIES:

- **Precalibrated Hall Probes**
  A wide selection of 1X, 10X and 100X precalibrated Hall probes are available to meet most applications.
- **Zero Gauss Chamber** (Model ZG-1)
  A mu-metal shield used to shunt the earth's field around the Hall element in order to more accurately zero the gaussmeter when precise low field measurements are required.
- **Reference Magnets**
  Transverse and axial precision reference magnets are available when precise instrument calibration at a particular field is desirable.

HALL EFFECT GAUSSMETERS

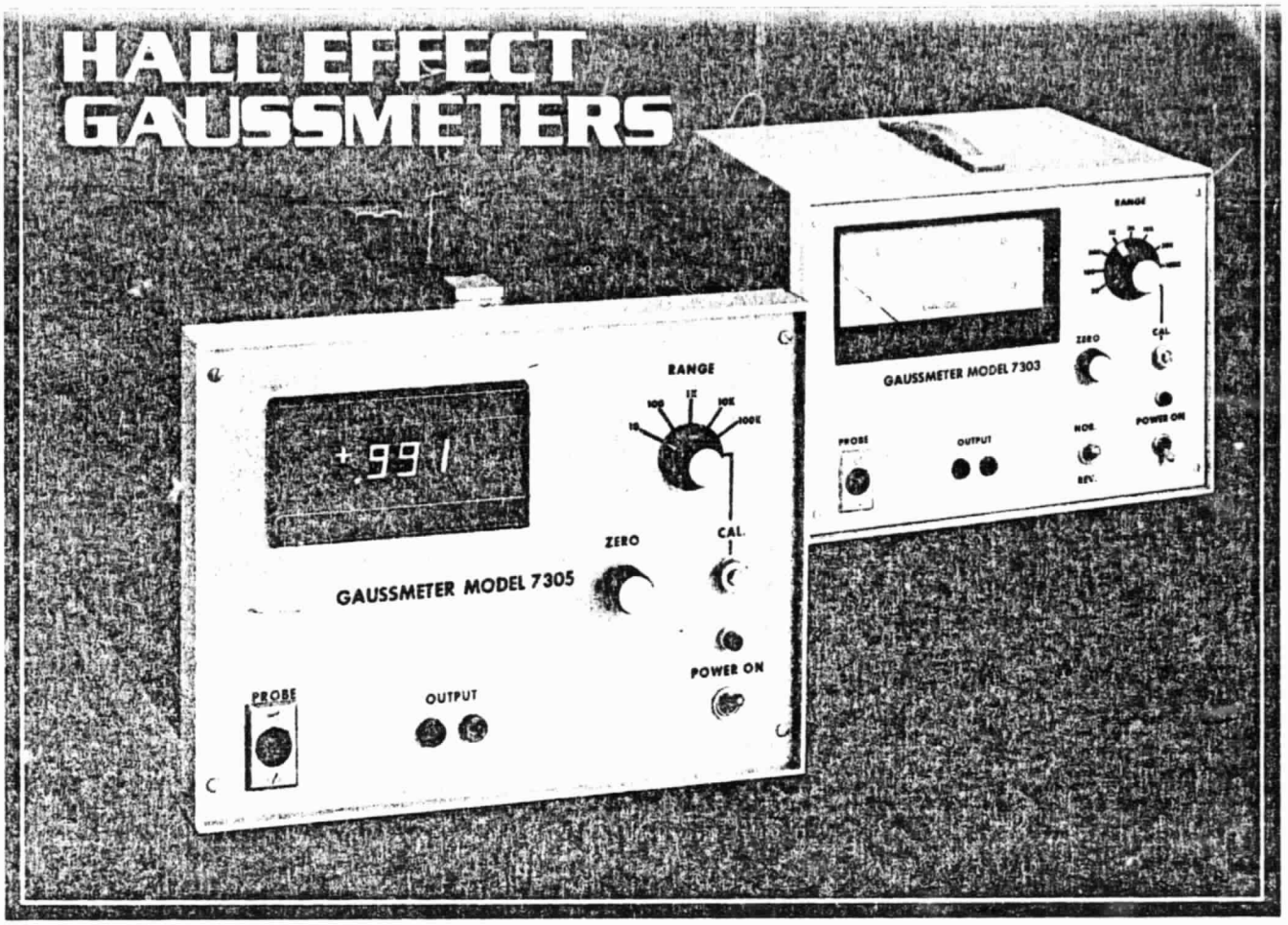

magnetic instrumentation inc.

FEATURES

- Magnetic field measurements from 1 Gauss (10^{-4} Tesla) to 100,000 Gauss (10 Tesla).
- Solid state circuit design.
- AC field response to 1 MHz.
- Accurate internal calibration.
- Simple setup and operation.
- 3½ digit panel meter or large taut-band mirror scale meter.
- Wide range of high linearity Hall probes.
- All controls on front panel.
- Output voltage accurate to 10X over range.

DESCRIPTION

The Models 7303 and 7305 Gaussmeters are high accuracy, wide range, stable magnetic flux density measuring instruments. Hall element probes are easily interchanged using the internal calibration feature of the Gaussmeter. Directional sensitivity is maintained through the Gaussmeter so that magnetic field polarity information is available for field plotting. Time varying magnetic fields up to 1 MHz can be measured using an external indicator. (Frequency response is dependent on range and Hall element.)

APPLICATIONS

The Models 7303 and 7305 Gaussmeters are easily adapted to engineering, quality control and production flux density measurements of permanent magnets, electro-magnets, loudspeakers, TWT magnets, magnetrons, PM motors, linear actuators, relays and other devices where an AC or DC magnetic field is encountered. Measurements made using the Models 7303 and 7305 can be used to determine the efficiency of a magnetic circuit, plot flux leakage paths of magnetic assemblies and evaluate the residual field of magnetic devices.

SPECIFICATIONS

MODEL 7303
ANALOG HALL EFFECT GAUSSMETER
RANGE
30 Gauss to 100,000 Gauss FULL SCALE in 8 ranges.
METER REPEATABILITY
0.5%
MODEL 7305
DIGITAL HALL EFFECT GAUSSMETER
RANGE
10 Gauss to 100,000 Gauss FULL SCALE in 5 ranges.
METER REPEATABILITY
0.1% R ± .05% of full scale.
MODELS 7303 and 7305
ACCURACY
Range switching error is 0.25% of full scale. The range switching error can be eliminated by calibrating the instrument on the range to be used with a reference magnet.
Internal calibration accuracy is 0.5%
Hall probes with 0.1% linearity over specified ranges are available.
Probe linearity should be considered when making precision measurements. (Consult probe data sheets for individual probe linearity specifications.)
OUTPUT
The voltage output jacks provide a 0 to ± 1 volt output for full scale range proportional to magnetic field at the probe.
POWER
120 volts ± 10%, 50/60 Hz, 30 watts
DIMENSIONS
8.2" high, 11.1" wide, 11" deep. (200 mm × 180 mm × 180 mm)
WEIGHT
Net 10 pounds. Shipping 15 pounds. (4.8 Kg., 7.1 Kg.)

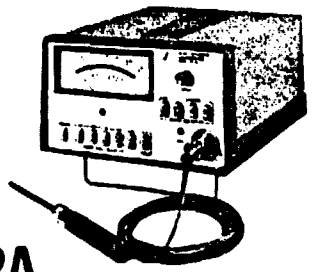

MG-2A

The MG-2A has eight full-scale ranges from 10 gauss to 30,000 gauss displayed on a taut-band mirror scale analog meter with zero center or zero left and becomes fully portable when supplied with the optional rechargeable battery pack indentical to MG-3A. A ± 1V ± 0.25% full scale analog output is also provided.

A unique feature of this instrument is that AC field measurements to 4000 Hz are made independent of DC field levels which allow AC fields to be measured in the presence of DC fields.

Specifications

RANGE 8 Full scale: 10, 30, 100, 300, 1K, 3K, 10K, 30K

VISUAL DISPLAY
- TYPE Analog, ± 1% taut-band mirror scale analog meter
- RANGE Zero left: 0-1 and 0-3
  Zero center: 1-0-1 and 3-0-3 for bipolar operation
- AC FIELDS Meter displays average rectified value of alternating flux density; ± 3% of full scale within frequency response range.
- FREQUENCY RESPONSE - DISPLAY
  - DC Mode DC to 1000 Hz on 10 and 30 gauss range
    DC to 4000 Hz on 100 through 30K gauss range
  - AC Mode 25 Hz to 1000 Hz on 10 and 30 gauss range
    25 Hz to 4000 Hz on 100 through 30K gauss range

OUTPUT:
- ANALOG VOLTAGE ± 1 V full scale and ± 3 V full scale on 3X range, over-range to ± 10 V without loss of data.
- ACCURACY - DC ± 0.25%
- ACCURACY - AC The voltage at the output terminals is proportional to the instantaneous AC field to within 1% of the output frequency response range
- FREQUENCY RESPONSE - OUTPUT
  - DC Mode DC to 1000 Hz on 10 and 30 gauss range
    DC to 4000 Hz on 100 through 30K gauss range
  - AC Mode DC to 1000 Hz on 10 and 30 gauss range
    DC to 4000 Hz on 100 through 30K gauss range
- OUTPUT IMPEDENCE 100 ohms
- LOAD IMPEDENCE Minimum of 1,000 ohms, short circuit protected

POWER INPUT: Approximately 6 Watts. .06 amps @ 105 V to 125 V or .03 amps @ 210 V to 250 V - 50 Hz to 400 Hz
- STANDARD 115 V, 50 Hz to 400 Hz
- OPTIONAL
  a) 220 V 50 Hz to 400 Hz
  b) Internal rechargeable batteries. Usable for 8 hours without recharging

PHYSICAL:
- SIZE $4\frac{3}{4}$" high x $8\frac{3}{4}$" wide x $11\frac{3}{8}$" deep
- WEIGHT 12 lbs. net, 18 lbs. shipping

EXPENDITURES

Grant NAS5-26414

As of 8/31/82

BALANCE SHEET

Salaries (P.I.) Services	$ 987.86
Travel	507.91
Publications	2,310.00
Maintenance	1,095.50
Supplies	316.59
Administrative	4,119.99
Equipment	539.33
Rental Computer	1,000.00
GRANT BALANCE	$10,877.18
Less negative overhad balance	1,125.22
	$ 9,751.96